



RSEN-RFF: Deep Learning-Based RF Fingerprint Recognition in Noisy Environment

Zhaonan Du¹(✉), Di Liu¹, Jiawen Zhang², Di Lin¹, Yuan Gao³, and Jiang Cao³

¹ School of Information and Software Engineering, The University of Electronic Science and Technology of China (UESTC), Chengdu, People's Republic of China
201922090507@std.uestc.edu.cn

² National Key Laboratory of Science and Technology on Communications, University of Electronic Science and Technology of China (UESTC), Chengdu, People's Republic of China

³ Military Academy of Sciences, Beijing, China

Abstract. As an emerging technology of Internet of Things security, radio frequency (RF) fingerprint identification technology can be used to identify wireless devices and meet the needs of the Internet of Things regarding user access control. Machine learning and deep learning have been applied to recognize a mobile device by extracting and analyzing its RF fingerprinting characteristics due to their powerful feature learning and representational abilities. However, the performance and accuracy of the learning algorithm will degrade dramatically in the circumstances of high-intensity noise (low signal-to-noise ratio, low SNR). To address this problem, this paper proposes an attention-based residual network algorithm, named RSEN-RFF, to train and recognize the RF fingerprint characteristics of lightweight mobile devices, and compared the proposed algorithm with classic convolutional neural networks (LeNet5, etc.), which are the most widely used algorithms for IoT device identification. Unlike other machine learning methods based on feature engineering, deep models use neural networks to solve the characterization of RF fingerprint features without the need for a process of feature extraction based on professional knowledge. The results show that the fitting speed and recognition accuracy of proposed algorithm are better than those of the previous algorithm under the condition of low SNR.

Keywords: RF fingerprint recognition · IoT security · Deep learning

1 Introduction

In recent years, with the rapid development of wireless networks, artificial intelligence and big data analysis technology, all kinds of Internet of things applications continue to emerge, becoming one of the three major application scenarios in the fifth-generation mobile communication network (5G) [1]. Online mobile devices and sensor deployments explosive growth. According to Cisco's forecast, there will be more than 25 billion terminal devices connected to each other through the Internet of Things in 2021 [2]. With the continuous expansion of the application scope of the Internet of Things and

the rapid growth of the number of devices, its security issues have become increasingly prominent. At present, the identification technology of wireless devices mainly includes traditional password-based methods. These methods mainly use IP, MAC addresses, etc. as the basis for identification [3], or use complex mathematical operations, protocols to generate keys, passwords, digital signatures, etc. to complete the identification work between users [4]. However, this method has hidden dangers such as key information leakage and tampering. Nowadays, the continuous improvement of computer capabilities has also made the ability to decipher passwords continuously enhanced, thus threatening the effectiveness of password-based identification methods. In addition, the Internet of Things devices includes a large number of lightweight devices, whose computing power cannot meet this complex identification method. Therefore, the method of purely using encryption becomes no longer reliable, and it is necessary to find a more stable and secure wireless device identity authentication method. In this context, RF fingerprint technology has become an emerging identity authentication method. It can identify the unique characteristics of the mobile device by analyzing the signal sent by the mobile device, thereby effectively preventing malicious parties from fake identity to obtain security credentials.

In a practical application scenario, there are various noises and interferences, such as multi-user co-channel interference and multipath interference. In a low SNR environment, the decay of SNR will conceal the small differences between devices, causing the fingerprint recognition rate of the device to drop significantly. Existing machine learning algorithms may not be suitable for radio frequency fingerprint identification with a low signal-to-noise ratio. Therefore, radio frequency fingerprint identification algorithms based on traditional machine learning or convolutional networks may reduce about 10%–20% at a signal-to-noise ratio of 5 dB performance [5]. This paper focuses on the research of radio frequency fingerprint recognition under the conditions of high-intensity electromagnetic noise. Based on the attention mechanism in deep learning that has been widely used in recent years, the residual module is introduced at the same time, and the cross-layer identity path of the residual network is adopted to alleviate the training difficulty of the deep network and improve the representation feature learning ability of the recognition model. In addition, the soft threshold function noise reduction algorithm in communication is used for reference, and the corresponding processing process is added to the model to eliminate the influence of SNR decay as much as possible. While improving the recognition accuracy, the overall generalization ability of the model is improved.

The rest of this paper is arranged as follows. Section 2 reviews the field of RF fingerprinting recognition and related learning methods. Section 3 describes the internal hardware impairments and channel models that lead to signal differences. Section 4 presents our methodology on RSEN-RFF based algorithm, followed by Sect. 5 which reports the simulation results. Section 6 concludes with a discussion of the results and suggestions for future research.

2 Related Work

The mainstream RF fingerprint identification technology mainly includes two research directions: one is feature-based RF fingerprint identification, and the other is data-based RF fingerprint identification. Feature-based RF fingerprint identification requires the combination of feature engineering and professional communication knowledge to extract appropriate device fingerprints, and then use the feature similarity between devices for identification. Specifically, traditional machine-learning algorithms are used to recognize the devices based on the device's unique fingerprint. Data-based RF fingerprint identification uses deep learning algorithms, which can automatically train the raw data of the signal to identify mobile devices.

Before 2018, the research of radio frequency fingerprint identification mainly focused on the use of machine learning algorithms, e.g., the support vector machines (SVM) algorithms are used to recognize the identity document (ID) of each mobile device. Some studies employ multi-core SVM algorithms to identify the ID of mobile devices, including Platt's Minimization Optimization (SMO) algorithms, the poly-kernel algorithms, and the Pearson-VII Universal Kernel (PuK) algorithms [6]. Generally, the PuK algorithms are more effective in RF fingerprint identification, obtains higher recognition performance, and greatly reduces calculation time. The traditional machine-learning RF fingerprinting identification technology first preprocesses the collected signals, including power normalization, noise reduction and label set. Then, the RF fingerprint characteristics are extracted from the pre-processed signal data through different algorithms, and the marked characteristics are stored in the fingerprint library. Finally, the extracted RF fingerprint features are used to identify the mobile devices. In the traditional machine-learning recognition technology, the key is to select appropriate signal characteristics from RF fingerprints.

After 2018, research on the application of deep learning in the field of RF fingerprint identification has gradually emerged. Sankhe et al. in [7] proposed to use a 2-layered convolution neural network (CNN) to train the RF fingerprinting data from 16 X310 USRP SDRs. Wu et al. in [8] employ a deep neural network (DNN) with a rectified linear units (ReLU) to run the training model for the RF fingerprint identification of 12 Ettus USRP N210. In addition, Wu et al. [8] proposed a neural network based on incremental learning to train data in multiple stages, and use new-arrival data to modify the learning model to speed up the training process. Compared with traditional feature extraction algorithms based on machine learning, RF fingerprint identification based on deep learning does not require feature extraction. After preprocessing, the predicted label is directly compared with the label registered in the fingerprint library in the deep learning network to identify different mobile devices.

In this paper, we use deep learning algorithms instead of machine learning to identify mobile devices. The RF signal of the device is represented by the original I/Q data. Assuming that we choose to use traditional machine learning algorithms, we must go through a complex feature selection process to construct a series of mathematical and statistical indicators. This process is time-consuming, and a lot of information can be lost. Therefore, we finally use deep learning algorithms to build learning models to distinguish transmission devices.

3 The Mechanism of RF Fingerprint Generation

3.1 RF Impairments and I/Q Imbalance

RF fingerprints are mainly caused by differences in hardware during the manufacturing process, including power amplifier defects, amplitude and phase errors, carrier frequency differences, phase offsets and clock offsets, etc. [9]. I/Q imbalance is a phenomenon that occurs in direct down-conversion radio frequency receivers, which directly down-converts the RF signal to the baseband. The conversion process from baseband digital signals to radio frequency analog signals will have a unique impact on radio frequency signals. Therefore, individual identification of wireless devices can be realized based on these inherent, stable and unique signal characteristics. In this section, we will introduce and study the mechanism of the RF fingerprint generated by the modulator. By using different modulation schemes, subtle differences in modulator hardware can be collected.

3.2 I/Q Imbalance on Different Channel

Although most modern communication systems are affected by frequency-dependent IQ imbalance, for simplicity, frequency independence is usually assumed in the existing literature [10]. This article first assumes that IQ imbalance has nothing to do with frequency, and the modulated signal is transmitted through different channels (e.g., additive white Gaussian noise channel, AWGN), as follows:

Denote the ideal signal $s(t)$ at the transmitter as:

$$s(t) = \cos(2\pi f_0 t) x_i(t) - j \cdot \sin(2\pi f_0 t) x_q(t) \quad (1)$$

where $x_i(t)$ and $x_q(t)$ are baseband signals respectively in the I and Q path, f_0 is the fixed carrier frequency.

Due to the different degrees of damage to the hardware, compared with the ideal signal $s(t)$, the actual signal $\hat{s}(t)$ modulated by different devices may have slight differences in amplitude and phase. Hence, the baseband signals which through IQ imbalance modulator can be denoted as:

$$\hat{s}(t) = (1 + \Delta) \cos(2\pi f_0 t + \theta) x_i(t) - j \cdot \sin(2\pi f_0 \Delta t) x_q(t) \quad (2)$$

the transmitter's gain imbalance is represented by Δ , and the transmitter's phase imbalance is represented by θ , such that the ideal transmitter, with no IQ imbalance, has $\Delta = 0$ and $\theta = 0$.

In this paper, we use additive white Gaussian noise to simulate training samples that pass through the AWGN channel, as follows:

$$y(t) = \hat{s}(t) + n(t) \quad (3)$$

where $n(t)$ is a zero-mean white Gaussian noise process.

For Rayleigh fading channels, this paper uses the form of circular complex Gaussian random variables to model the tap coefficients as follows:

$$\alpha_k = A + j \cdot B \quad (4)$$

where α_k is the path index, A and B are zero mean iid Gaussian random variables with variance σ^2 [11] as follows:

$$\sigma^2 = \frac{1}{2} \left\{ \left[1 - \exp\left(\frac{-T_s}{T_{rms}}\right) \right] \exp\left(\frac{-kT_s}{T_{rms}}\right) \right\} \quad (5)$$

where T_s is the sampling period and T_{rms} is the Root-Mean-Squared (RMS) delay spread of the channel [11], and the Rayleigh channel model is defined as:

$$h(t, \tau) = \sum_{k=1}^L \alpha_k \delta(t - \tau_k T_s) \quad (6)$$

where τ_k is the delay of the k -th path normalized by T_s [12]. In summary, the modulated signal after passing through the Rayleigh fading channel is as follows:

$$r(t) = \hat{s}(t) * h(t, \tau) + n(t) \quad (7)$$

where $*$ denotes convolution.

In the following, we will use the subtle difference between the ideal signal and the actual signal as the internal features of mobile devices to identify them. We use different channel conditions, e.g. (3), (6) and (7) to simulate the real environment, and using the amplitude difference and phase difference in (2) to distinguish between different devices, which will be shown in Sect. 6.

4 Network Structure

In this section, the design and training approaches of the Residual Squeeze-and-Excitation Networks for the RF fingerprint (RSEN-RFF) are introduced. The RSEN-RFF network in this paper trains IQ samples of radio frequency signals to identify IoT devices. It is an improved residual network based on the channel attention mechanism. It consists of typical components, such as a convolutional layer, batch normalization (BN), rectification linear unit (ReLU), global average pool (GAP), fully connected layer (FC). The innovation of this article in the deep network is mainly reflected in the residual building unit (RSBU) we proposed with reference to the residual-based channel attention mechanism. The structure of RSEN-RFF is shown in Fig. 1.

4.1 Design of Essential Architectures of RSEN-RFF

The most important component of a convolutional neural network is the filter that performs convolution operations in the convolutional layer. Because the convolution operation can describe image features well, it is widely used in image recognition tasks. In this paper, the convolutional layer is used to abstract RF fingerprint features, by calculating the convolution between the input initial I/Q sample and the convolution kernel, the convolution layer is used to abstract and extracts the RF fingerprint features, which can compress the input data size to reduce the space complexity of the model. RSBU is the core of the RSEN-RFF model, which can suppress noise components by using dynamic thresholds. Generally, RSBU consists of one layer of BN, one convolutional layer with

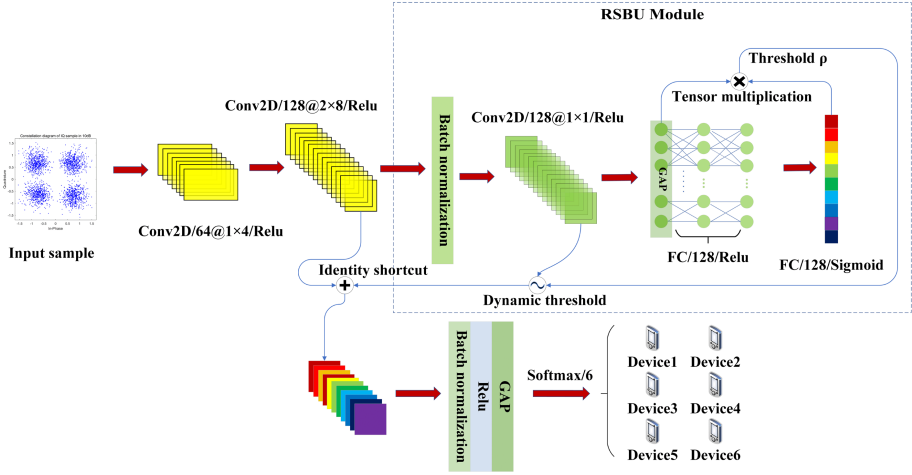


Fig. 1. The overall architecture of RSEN-RFF

rectifier linear unit, one layer of GAP, three layers of FC. Among all fully connected layers, the first two use the ReLU activation function, and the third layer uses the sigmoid activation function. BCR includes three components, namely batch normalization (BN), rectifier linear unit (ReLU) and convolutional layer unit. BCR assumes the role of nonlinear transformation, improves the deep abstraction ability of the network, and further expands the characterization of the RF fingerprint characteristics in I/Q samples. The GAP layer calculates the mean value of the characteristic channel as the input of the channel weight calculation.

4.2 Dynamic Threshold

Soft thresholding is often used as a key step in many signal denoising methods. Usually, the original signal will be scaled, and then soft thresholding will be applied to convert the features close to zero into zero. However, the setting of the soft threshold has always been a challenging problem. Deep learning provides a new way to solve this problem. Deep learning can use the gradient descent algorithm to automatically learn the filter threshold, instead of artificially setting the threshold by expert experience. Therefore, the integration of soft thresholds and deep learning can be a promising method to eliminate noise-related information and build highly discriminative features. The function of the soft threshold can be expressed as:

$$y = \begin{cases} x - \rho, & x > \rho \\ 0, & -\rho \leq x \leq \rho \\ x + \rho, & x < -\rho \end{cases} \quad (8)$$

where x represents the features of input I/Q signals, y represents the output features, and ρ represents a dynamic threshold which is usually a positive parameter. Different from the ReLU activation function, the soft threshold setting is not to set the negative feature

to zero, but to set the feature close to zero, so that the useful negative feature can be retained.

The used in the RSBU is expressed as follows:

$$\rho = \omega \Delta \text{mean}[|x|] \quad (9)$$

where $\text{mean}[|x|]$ represents the mean of input x , and ω represents the scaling parameter, which is expressed as:

$$\omega = (1 + e^{-t})^{-1} \quad (10)$$

where t represents the output of fully connected networks.

4.3 The Structure of RSBU

RSBU is an improvement based on SENet [13] and residual network. It uses a dynamic threshold method to suppress noise components and inserts the dynamic threshold as a nonlinear conversion layer into the building unit. In addition, the threshold can be trained in the building unit, which will be described below.

As shown in Fig. 1, In the RSBU module, the input data is IQ samples that have been convolved twice, and the output data is the data that has undergone a dynamic threshold filtering operation and a residual cross-layer identity shortcut operation. First, the input data by BN layer, in order to address after two convolution data distribution changes, in order to prevent the disappearance or explosion gradient, speed up the training. Then there is a convolutional layer to further abstract the channel features of the feature map. Since this layer performs a residual cross-layer identity shortcut operation with the input data after dynamic threshold filtering, the size of the feature map here needs to be aligned. Common alignment methods include a 1×1 convolution kernel and zero paddings. This paper uses a 1×1 convolution kernel for feature map alignment. The following is the generation and filtering of dynamic thresholds. The feature map obtains a one-dimensional vector of the channel average value through the GAP layer. Then, the one-dimensional vector is propagated to the three-layer full-path network, and a sigmoid function is applied at the end of the full-path network to scale the scaling parameter ω to the range of (0,1). The scaling parameter is as shown in formula (10) above. The scaling parameter is multiplied by the channel average value to obtain the dynamic threshold ρ vector, as in the above formula (9). Finally, use the dynamic threshold vector to filter the feature map, and output the data after the cross-layer identity shortcut operation.

After being processed by the RSBU module, the sample data has been greatly abstracted and noise suppressed. The conventional BCR layer and Softmax function can be used to classify and identify the device.

5 Simulation Experience

5.1 Data Sampling Platform

We built a data sampling platform in a static indoor office environment, as shown in Fig. 2. The IQ sequences used in this paper, including the training data and the test

data, are collected from Universal Software Radio Peripherals (USRPs). Our hardware platform consists of NI-PXIe 1085 devices and two USRP-RIO-2943. NI-PXIe 1085 is a computer-based platform for data transmission and graphic display. All transmitters of the RIO2 are bit-similar and emit IEEE 802.11a standards compliant frames generated via a MATLAB WLAN System toolbox. We use the open-source GNU Radio companion (GRC) to transmit standard-compliant IEEE 802.11a data packets through the SDR. Using `set_iq_balance()` and `set_dc_offset()` functions in GRC, these two separate complex correction factors can be set to intentionally introduce required level of impairments in the radio. By the above methods, we simulate six different transmitters that need to be identified; The other USRP RIO-2943 (RIO1) is a fixed receiver, responsible for receiving signals from the six transmitters. As for the transmitters, their hardware differences can lead to amplitude difference and phase difference. We will set the parameters as follows: signal impairment transmitter only has an offset 1 in amplitude, a signal transmitter 2 only has offset damage in phase, the remaining transmitter mode offset exists in amplitude and phase.

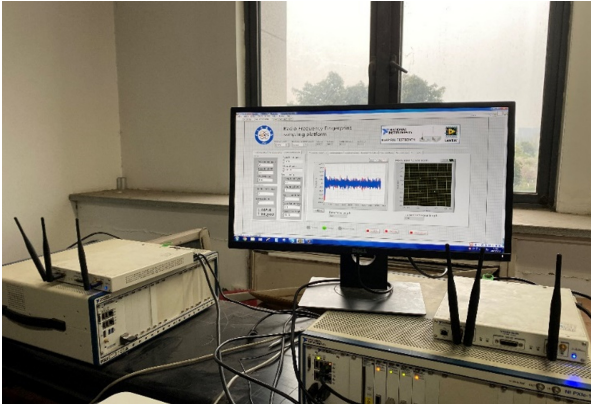


Fig. 2. Signal sampling platform for data collection.

5.2 Data Pre-process

The data samples sent to the network in the past are all original I/Q two-way signals, in which the signals are generated by modulating different phases and amplitudes according to a randomly generated bitstream. In training and testing above 15 db, the order of the bitstream has little effect on the recognition result, and training using the original I/Q two-way signal is text-independent. However, under the condition of a low SNR, the obvious text correlation appears during training, that is, the effect of training and testing with different batches of bitstreams is not good. In order to eliminate the influence of the sequence under the condition of a low SNR, consider rearranging the original I/Q two-way signals and then sending them to the network for training. Taking QPSK modulation as an example, we can separate the four I/Q signals representing 00 01 10 11, and then

sort them, and rearrange the original $2 \times N$ size I/Q signals into $8 \times N/4$ format. The schematic diagram of QPSK modulation rearrangement is shown in Fig. 3:

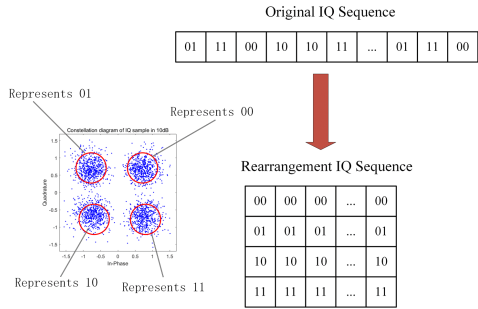


Fig. 3. IQ data sample rearrangement diagram

5.3 Experiment I: Effects of Different Modulation Identification Rearrangement

In this experiment, we compared the impact of the rearrangement preprocessing method under different modulation methods on the recognition accuracy under the AWGN channel. As shown in Fig. 4, the overall recognition accuracy after rearrangement can be improved by about 5%–20%. In addition, in PSK modulation, as the phase point increases, the accuracy of the radio frequency fingerprint will decrease to a certain extent, but the rearrangement preprocessing can effectively solve this problem. In Fig. 4, without pre-processing, the recognition accuracy difference between BPSK, QPSK and 8PSK modulation methods is about 5%–10%. This gap can be reduced to 1%–3% after rearrangement and preprocessing. Rearrangement is a key step to eliminate the relevance of text content. All results are executed based on the RSEN-RFF algorithm, which shows that our network is robust to the reordering pre-processing under the modulation mode. According to the results of the experiment, the rearrangement preprocessing of IQ samples can effectively improve the recognition accuracy of the network and is not affected by the modulation method.

5.4 Experiment II: Effect of Different Conditions Identified Rayleigh Channel

Multipath seriously affects the performance of a wireless communication network, because destructive interference will produce a plurality of reflected signals received at the receiver. This is the main problem between 802.11a wireless transceivers in the indoor environment [14]. The paper simulates the Rayleigh fading channel model to collect IQ sample data in the indoor multipath environment. At this time, there are one or more paths without a line path. The Rayleigh fading channel model is a standard method for predicting IEEE 802.11a WiFi modulation performance in a wireless multipath environment. Multipath is characterized by the time delay associated with each reflection path and is called delay spread. The delay spread varies based on the type

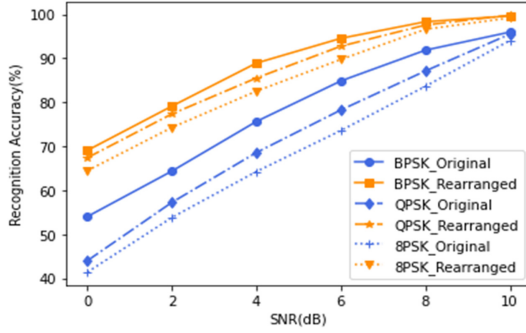


Fig. 4. Accuracy comparison of different modulation identification rearrangement

of indoor environment. For example, the delay spread is lower than 50 ns in a home multipath environment, and about 100 ns in an Office environment. The modeling of the Rayleigh fading channel is represented by the above formula (4)–(7).

In order to test the robustness of the model under complex conditions, we designed and simulated a set of parameters under different Rayleigh fading channel conditions, as shown in Tables 1 and 2, where the channel conditions become worse as the number of paths increases. The channel estimation adopts the least-squares (LS) channel estimation, and the channel equalization adopts the minimum mean square error (MMSE) equalization.

Table 1. Delay selection of different paths $T_{RMS} = 100$

Path delay															
L	50	100	150	200	250	300	350	400	450	500	550	600	650	700	750
3	✓	--	✓	--	✓	--	--	--	--	--	--	--	--	--	--
5	✓	--	✓	--	✓	--	✓	--	✓	--	--	--	--	--	--
7	✓	✓	--	✓	✓	--	✓	--	✓	--	✓	--	--	--	--

Table 2. A normalized variance of fading coefficients for different paths $T_{RMS} = 100$

Path variances (σ_k^2)													
L	50	100	150	200	250	300	350	400	450	500	550	600	
3	0.6652	--	0.2447	--	0.0900	--	--	--	--	--	--	--	--
5	0.6364	--	0.2341	--	0.0861	--	0.0317	--	0.0117	--	--	--	--
7	0.4153	0.2519	--	0.0927	0.0562	--	0.0207	--	0.0076	--	0.0028	--	--

By evaluating the recognition accuracy of the RF fingerprint feature in the Rayleigh fading channel, as shown in Fig. 5, the average recognition accuracy fluctuates within 7% under different Rayleigh fading channel conditions, indicating that the RSEN-RFF algorithm has a good generality. It can overcome the influence of signal fading in the actual environment on the accuracy of radio frequency fingerprint identification. At the same time, when the signal-to-noise ratio is greater than 6 dB, the average recognition accuracy of the RSEN-RFF algorithm on the Rayleigh fading channel test samples can reach more than 85%.

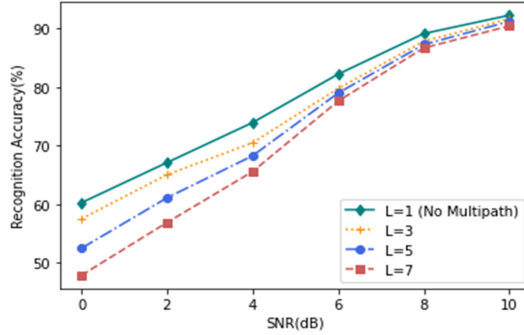


Fig. 5. Accuracy comparison of different conditions identified Rayleigh channel

5.5 Experiment III: The Proposed RSEN-RFF V.S. LeNet5

In this experiment, we compare the convergence speed and accuracy of RF fingerprint identification with LeNet5 and our RSEN-RFF algorithm. As shown in Fig. 6, the average recognition accuracy of the RSEN-RFF algorithm is higher than that of LeNet5 by about 15%–20%. In terms of convergence speed, as shown in Fig. 7, when the SNR is greater than 6 dB, RSEN-RFF needs 8–9 epochs to achieve AWGN channel convergence, while LeNet5 requires 18–20 epochs to achieve convergence.

In addition, when the SNR is less than 6 dB, it takes more than 12 epochs to achieve the convergence of the Rayleigh channel in RSEN-RFF, and 20 epochs to converge in LeNet5. The reason is that, compared with the AWGN channel, the Rayleigh fading channel is affected by the multipath effect, so it needs more time to learn the characteristics of the signal.

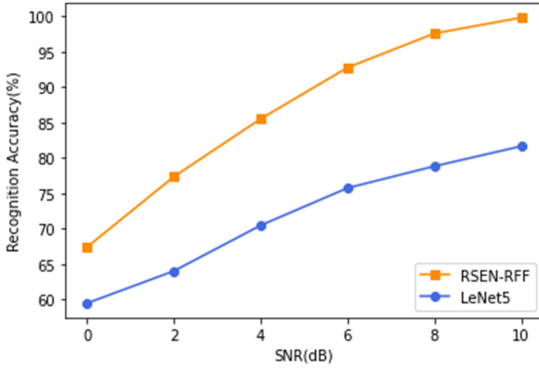


Fig. 6. Accuracy comparison of RSEN-RFF and LeNet5

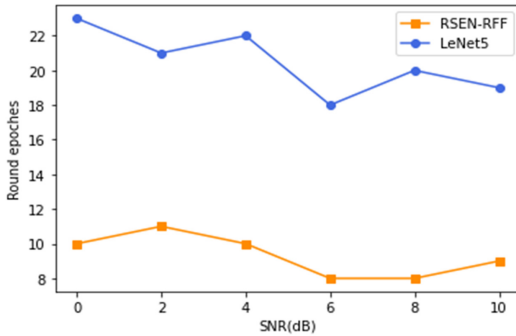


Fig. 7. Convergence and round epochs comparison of RSEN-RFF and LeNet5

6 Conclusion

In this paper, we propose RSEN-RFF, which is a novel algorithm to identify IoT devices via RF fingerprint analysis. RSEN-RFF can effectively overcome low SNR settings in some IoT scenarios. Specifically, our algorithm incorporates a dynamic shrinkage threshold to improve the accuracy of device recognition. In addition, compared to traditional methods, RSEN-RFF can accelerate the training process of model learning. Detailed analysis and extensive experiments have proved the robustness of RSEN-RFF in various SNR scenarios. Finally, the actual deployment of the six-device network shows that in terms of recognition accuracy and running time, RSEN-RFF is overall better than the typical CNN network LeNet5, thus meeting the security requirements in real-time IoT scenarios. In order to further improve the robustness of the network in complex situations, we plan to extend the scope of research to the case of small-scale sampling data, in which case the amount of data is insufficient for model training. In actual situations, the number of RF signals collected by a single device may be unbalanced.

Acknowledgement. Partially Funded by Science and Technology Program of Sichuan Province (2021YFG0330), partially funded by Grant SCITLAB-0001 of Intelligent Terminal Key Laboratory of SiChuan Province, and partially Funded by Fundamental Research Funds for the Central Universities (ZYGX2019J076).

References

1. Li, S., Xu, L.D., Zhao, S.: 5G Internet of Things: a survey. *J. Ind. Inf. Integr.* **10**, 1–9 (2018)
2. Zhang, K., et al.: Sybil attacks and their defenses in the internet of things. *IEEE Internet of Things J.* **1(5)**, 372–383 (2014)
3. He, D., Zeadally, S.: An analysis of RFID authentication schemes for internet of things in healthcare environment using elliptic curve cryptography. *IEEE Internet Things J.* **2(1)**, 72–83 (2014)
4. Zhao, F., Jin, J.: An optimized radio frequency fingerprint extraction method applied to low-end receivers. In: 2019 IEEE 11th International Conference on Communication Software and Networks (ICCSN). IEEE (2019)
5. Peng, L., et al.: Deep learning based RF fingerprint identification using differential constellation trace figure. *IEEE Trans. Veh. Technol.* **69(1)**, 1091–1095 (2019)
6. Hu, S., et al.: Machine learning for RF fingerprinting extraction and identification of soft-defined radio devices. In: Liang, Q., Wang, W., Mu, J., Liu, X., Na, Z., Chen, B. (eds.) *Artificial Intelligence in China. Lecture Notes in Electrical Engineering*, vol. 572, pp. 189–204. Springer, Singapore (2020). https://doi.org/10.1007/978-981-15-0187-6_22
7. Sankhe, K., et al.: ORACLE: optimized radio classification through convolutional neural networks. In: IEEE INFOCOM 2019-IEEE Conference on Computer Communications. IEEE (2019)
8. Wu, Q., et al.: Deep learning based RF fingerprinting for device identification and wireless security. *Electr. Lett.* **54(24)**, 1405–1407(2018)
9. Ding, G., Huang, Z., Wang, X.: Radio frequency fingerprint extraction based on singular values and singular vectors of time-frequency spectrum. In: 2018 IEEE International Conference on Signal Processing, Communications and Computing (ICSPCC). IEEE (2018)
10. Wong, L.J., Headley, WC., Michaels, A.J.: Emitter identification using CNN IQ imbalance estimators. arXiv preprint [arXiv:1808.02369](https://arxiv.org/abs/1808.02369) (2018)
11. O'hara, B., Petrick, A.: IEEE 802.11 Handbook: A Designer's Companion. IEEE Standards Association, Piscataway (2005)
12. Hijazi, H., Ros, L.: Polynomial estimation of time-varying multipath gains with intercarrier interference mitigation in OFDM systems. *IEEE Trans. Veh. Technol.* **58(1)**, 140–151 (2008)
13. Hu, J., Shen, L., Sun, G.: Squeeze-and-excitation networks. In: Proceedings of the IEEE Conference on Computer Vision And Pattern Recognition (2018)
14. Fadul, M., et al.: Preprint: using RF-DNA fingerprints to classify OFDM transmitters under rayleigh fading conditions. arXiv preprint [arXiv:2005.04184](https://arxiv.org/abs/2005.04184) (2020)